

# Optimization of Induction Machine Design for Electric Vehicle Powertrain

1<sup>st</sup> Meng Lu

Division of Industrial Electrical  
Engineering and Automation  
Lund University  
Lund, Sweden  
meng.lu@iea.lth.se

2<sup>nd</sup> Gabriel Domingues-Olavarria

Division of Industrial Electrical  
Engineering and Automation  
Lund University  
Lund, Sweden  
gabriel.domingues@iea.lth.se

3<sup>rd</sup> Francisco J. Márquez-Fernández

Division of Industrial Electrical  
Engineering and Automation  
Lund University  
Lund, Sweden  
fran.marquez@iea.lth.se

4<sup>th</sup> Hannes Bydén

Division of Industrial Electrical  
Engineering and Automation  
Lund University  
Lund, Sweden  
hannes.byden@iea.lth.se

5<sup>th</sup> Mats Alakula

Division of Industrial Electrical  
Engineering and Automation  
Lund University  
Lund, Sweden  
mats.alakula@iea.lth.se

**Abstract**—This paper proposes a methodology to include induction machine (IM) in an optimization scheme for EV powertrains using Particle Swarm Optimization (PSO) as the optimization algorithm. The IM model is developed based on finite element analysis (FEA) and all the losses are estimated. The main objective is to generate a large database of base designs in a computationally efficient but accurate way. To perform the optimization, scaling methods are used. Detailed transmission and inverter models are also considered based on previous work to estimate the overall powertrain efficiency. The optimization case study shows how the optimizer evaluates a large number of alternatives and picks the optimal IM design and associated transmission and inverter. The proposed methodology can serve as a basis for future research on powertrain optimization for dual-motor driven vehicles.

**Keywords**— Induction machine, Powertrain optimization, loss estimation, PSO

## I. INTRODUCTION

The induction machine (IM) is considered as a cheap and robust option for electric vehicles traction. Induction machines typically benefit from having a lower number of poles, which also translates into a reduction in iron losses due to the lower electrical frequency, compared to an equivalent permanent magnet synchronous machine (PMSM). The main losses in the IM are the copper losses which lead to an extended high efficiency operation area towards the high-speed region, compared with PMSM [1].

In [1], a genetic algorithm for optimization of 3-phase induction motor is proposed, where the IM model is based on magnetic circuit analysis. In [2], the IM optimization is based on Rmxprt in Maxwell, parameters including rotor slot type, stator slot type, steel sheet and rotor material are optimized to obtain higher torque and efficiency.

To speed up the optimization, a scalable IM model is desired, in order to create a large enough design space as input to the optimization process. This approach was introduced in [3] for PMSM optimization. The initial PMSM database was built up using FE method beforehand. Selecting a "base" machine from the database, new machine designs can be generated with different scaling factors in limited computational time.

A properly designed transmission plays a crucial role in determining the efficiency and performance of the electric powertrain. In [4], a method to optimize the gear ratio selection of a single-speed electric vehicle drivetrain to reduce energy consumption is proposed. In [5], the loss model of transmission, together with electric machines, is developed to optimize the energy efficiency of different battery electric powertrain topologies.

Several studies focus on the development of comprehensive characterization and modelling for power semiconductors to optimize the traction inverter using Si and SiC devices [6][7].

This paper proposes a modification to the method presented in [3] in order to include IMs into the optimization of electric powertrains. As part of this methodology, a computationally efficient but accurate way of estimating and scaling the performance of IMs is described in detail. Building upon the work in [7], [8] and [9], the inverter and transmission model are adapted in this work.

## II. MODELING OF INDUCTION MACHINE

In this paper, a tool is developed in MATLAB, which uses FEMM to automatically generate finite element (FE) models of IMs. This tool allows for efficient exploration of parameter sensitivity analysis for IMs and can generate a large database of designs. The geometry of the IM is fully parametrized, and all dimensions can be easily modified through a user-friendly MATLAB interface. An example of one such IM model is presented in Fig. 1.

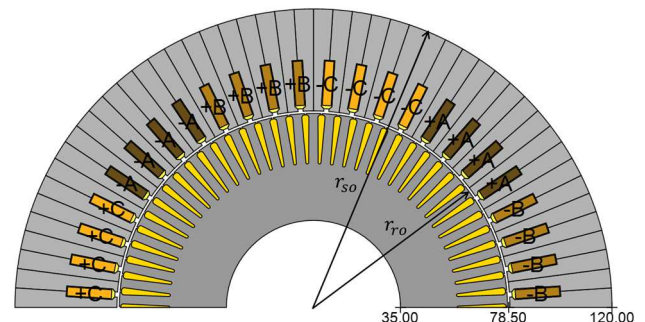


Fig. 1. Example of IM

The work is supported by Swedish Energy Agency.

The given figure depicts an IM with 48 stator slots and 4 poles.  $r_{so}$  is the stator outer radius and  $r_{ro}$  the rotor outer radius. It is possible to vary the stator slot size relative to the stator lamination. Additionally, the rotor comprises 74 copper bars, and the bar area can be adjusted to different values.

### A. Loss Estimation

The iron losses of an electrical machine can be categorized into three types: hysteretic loss, eddy current loss, and excess loss. Steinmetz's equation [10] can be used to calculate the iron loss of the IM, and is given by (1). The coefficients, namely  $k_{hyst}$ ,  $k_{eddy}$  and  $k_{exc}$ , can be derived from material datasheets, while the flux density data can be obtained from FE simulations.

$$P_{fe} = k_{hyst}fB^2 + k_{eddy}(fB)^2 + k_{exc}(fB)^{1.5} \quad (1)$$

The stator DC copper losses are calculated as shown in (2).  $R_{s\_act}$  is the resistance of the active length of the winding and  $R_{s\_end}$  the resistance of the end winding. The stator AC copper losses [3] can be estimated analytically by (3).

$$P_{cu\_DC} = 3I_s^2(R_{s\_act} + R_{s\_end}) \quad (2)$$

$$P_{cu\_AC} = \frac{1}{24}\sigma \cdot H^3 \cdot W \cdot hm \cdot \sum_{m=1,3,5,\dots}^{\infty} B_m^2 \cdot (m\omega_e)^2 \quad (3)$$

$H$  and  $W$  are the height and width of one conductor,  $hm$  is the active length of the electrical machine,  $\sigma$  is the conductivity of the conductor,  $B_m$  and  $\omega_e$  are the amplitude of the  $m$ -order harmonic for the leakage flux in tangential direction and electrical angular velocity of the first order harmonic of the leakage flux for this conductor, respectively.

The rotor bar copper losses can be directly collected from FE simulation results. The copper losses for the rotor end rings can be estimated by (4), assuming that the current density in the end ring and rotor bars are kept the same [11].

$$P_{cu\_r\_ring} = I_r^2 \cdot 4 \cdot \rho_{cu} \cdot r_{ro} \cdot N_{bar} / (N_p A_{bar}) \quad (4)$$

Where  $I_r$  is the induced current in the rotor bars,  $\rho_{cu}$  is the resistivity of copper,  $r_{ro}$  is the outer radius of the rotor,  $N_{bar}$  is the number of rotor bars,  $N_p$  is the number of poles,  $A_{bar}$  is the cross-sectional area of a single rotor bar and  $P_{cu\_r\_ring}$  represents the copper losses for the end ring.

### B. Control Algorithm

The stator current and slip frequency are used as input of FE simulations. The FE model performs a parameter scan on all input combinations. Then the FE model will calculate the magnetic field distribution and electromagnetic force within the machines, and subsequently generate output variables such as torque, flux linkage, flux density, and so on.

The torque and flux linkage contour map is then generated as a function of the stator current and slip frequency, as illustrated in Fig. 2. This provides a detailed visualization of

the IM's performance under various operating conditions.

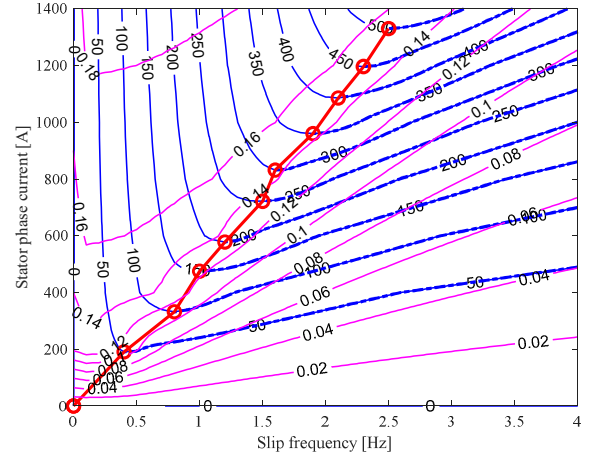


Fig. 2. Torque (blue) and flux linkage (pink) map; MTPA points (red circle)

It can be seen from Fig. 2 that the maximum torque per ampere (MTPA) points are picked as the operating points. Each of these optimal operating points is characterized by unique stator phase current and slip frequency values. The research objective of this paper is to optimize the powertrain based on the IM. Therefore, the estimation of IM parameters and current decoupling are beyond the scope of this research. With this method, it is feasible to directly extract the electromagnetic data from FE simulations. This enables the estimation of all losses, as illustrated in Fig. 3-5.

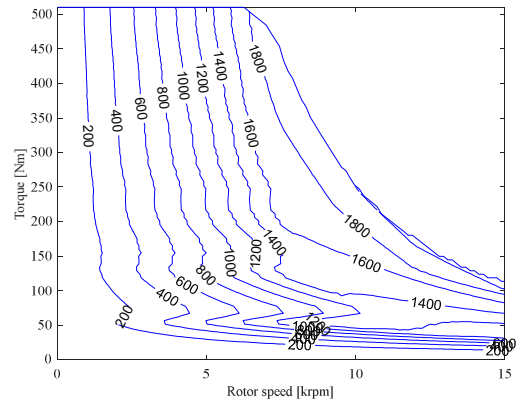


Fig. 3. Iron losses (W)

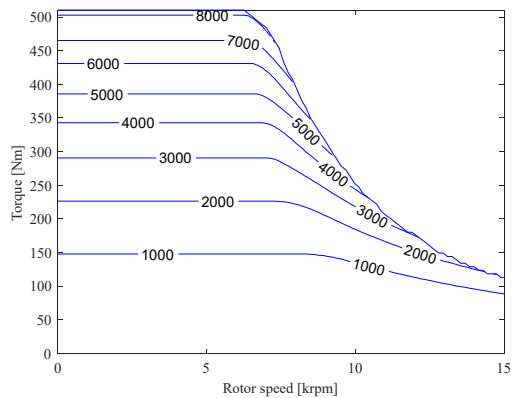


Fig. 4. Stator winding copper losses (W)

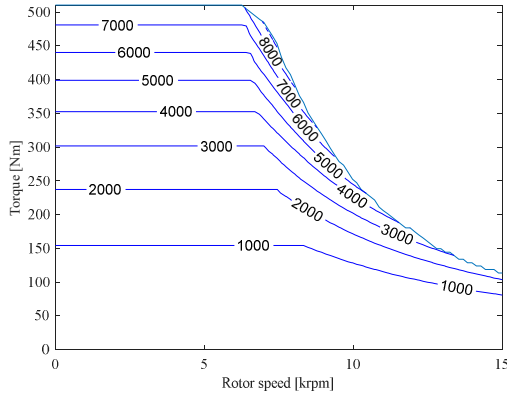


Fig. 5. Rotor copper losses (W)

### C. Scaling Method

After evaluating the performance and losses of the "base" IM model, a scaling method [12], [13] is introduced. This method is specifically designed for 2D FEM models and requires taking into account the effect of end winding when estimating the scaled machine. Given a DC-link voltage (750V in this paper), the scaling method recalculates the characteristics of the IM base model varying both the active length and number of winding turns. The IM performance is scaled based on two factors: the change in the EM axial length ( $k_a$ ) and the number of stator winding turns ( $N_t$ ).  $k_a$  is the ratio between the desired EM active length and the one set in FE simulation. The default value for the number of turns in the "base" IM model is set to 1. The scaling method provides a flexible and efficient way to explore a wide range of design options for IM optimization.

The effect of the scaling is described with

$$T, \psi_s, U_s, P_{cu,s,act}, P_{cu,r,act}, P_{fe} \propto k_a \quad (5)$$

$$U_s \propto N_t \quad (6)$$

Where  $T$  is the torque,  $\psi_s$  is the flux linkage,  $U_s$  is the induced voltage,  $P_{cu,s,act}$  is the stator copper losses for active part,  $P_{cu,r,act}$  is the rotor copper losses for active part,  $P_{fe}$  is the iron losses.

### III. MODELING OF TRANSMISSION AND INVERTER

A transmission model capable of accurately sizing each of the main component (gears, shaft and bearings) and calculating the corresponding efficiency and loss maps, has been developed for this work. The model has been validated using Masta and presented in detail in [9] but modified to be used in this optimization procedure. This model is capable of sizing single and multi-speed transmissions with parallel or transversal architectures and optimizes the gear ratio split between the different meshes as to minimize weight and energy consumption during cruising speed. Fig. 6 illustrates the model for designing and optimizing the transmission, while Fig. 7 depicts the layout of a two-stage single speed transmission.



Fig. 6. Transmission optimization model [9]

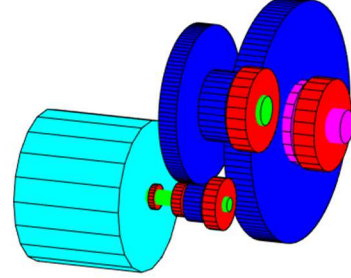


Fig. 7. Transmission layout

The inverter model is based on the study introduced in [7] [8] and SiC is selected as the power module. The loss calculation for the inverter is based on scalable electro-thermal models of power modules. The scalable resistance, on-state voltage and switching loss models were created by extracting data from manufacturer datasheets of several power modules from same generation and with the same packaging. The loss estimation process is presented in Fig. 8.

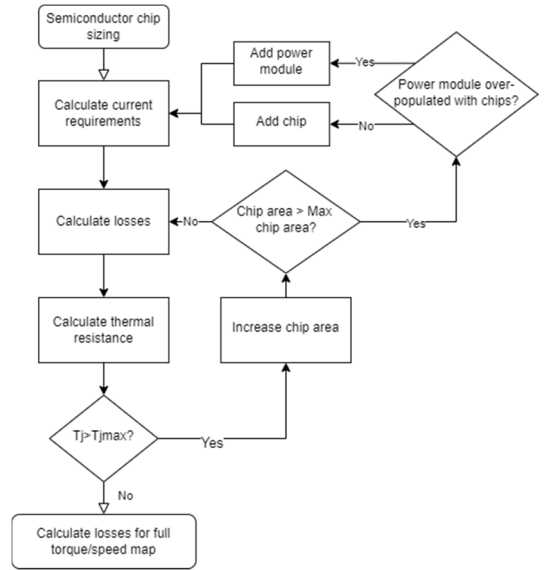


Fig. 8. Process of inverter loss estimation

Similar to the IM model described in this paper, the primary aim of these models is to offer a precise and computationally efficient characterization of the component's efficiency, size, and performance.

### IV. OPTIMIZATION PROCEDURE

The optimization process for the IM involves employing both the simulation and scaling methods as discussed earlier. To initiate the optimization, a database of various 2D geometries for the IM is required. By utilizing the parameterized values listed in Table I, a database comprising 900 distinct 2D IM geometries is generated.

TABLE I. IM DATABASE

Parameter	Values	Unit
$r_{so}$	240	mm
$r_{ro}/r_{so}$	[0.6 0.65]	-
Num. of poles	4	-
Num. of slots per pole per phase	[3 4 5]	-
Num. of rotor bars	[38 42...70 74]	-
Ratio between total area of bars and rotor	[0.1 0.12 0.14 0.15 0.16]	-
Relative slot size	[0.9 0.95 1]	-

### A. Definition of Vehicle Requirements

In this study, an EV powertrain with a single speed transmission and a single IM is considered. The specifications of the vehicle under study are presented in Table II.

TABLE II. VEHICLE SPECIFICATIONS

Parameter	Values	Unit
Weight	1480	kg
Front area	2.20	m <sup>2</sup>
Drag coefficient	0.31	-
Rolling resistance	0.008	-
Max speed	160	km/h
Acceleration 0-100kph	< 9	s
Overtaking 80-120kph	< 4	s
Gradeability	7% @160 km/h 25% @40 km/h	-

Based on the vehicle requirements listed in Table II, the required performance on wheel side is determined, as depicted in Fig. 9. The WLTP drive cycle is used in this study.

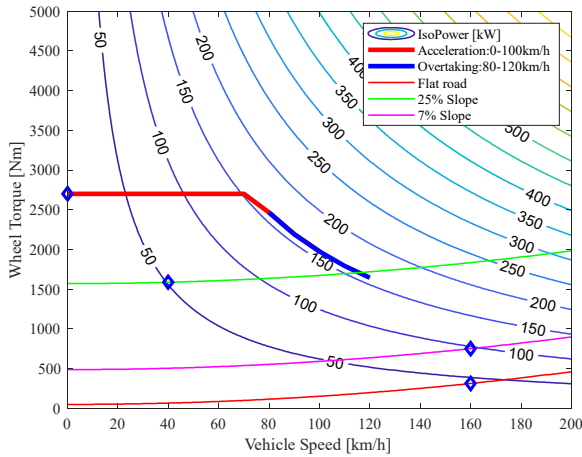


Fig. 9. Vehicle requirements

### B. Optimization Target

The optimization target is defined as the sum of two terms,  $C_{op}$ , which represents the operating cost of the vehicle and  $C_{IM}$ , which represents the cost of the induction machine.

$$C_{tot} = C_{op} \cdot k_c + C_{IM} \cdot (1 - k_c) \quad (7)$$

The weighting factor  $k_c$  is introduced to be able to prioritize between these two terms. The operating cost of the vehicle is estimated by the powertrain energy consumption over the course of one year, assuming an annual mileage of 20,000 km. The electricity price used in the calculations is set to 0.3€/kWh.

The IM cost model used in this study is derived from [14]. It includes the cost dependency on production volumes and the cost split within various manufacturing steps. Fig. 10 illustrates the relationship between the IM cost and the annual production volume. The yearly production volume is assumed to 100,000 units per year in this paper.

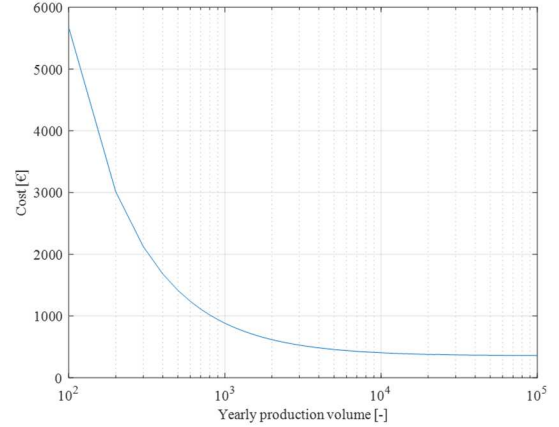


Fig. 10. IM cost vs production volume

### C. Optimization Methodology

First a certain IM geometry is selected from the database. This IM model (base motor) can be scaled to generate new machines by adjusting two scaling factors as previously described:  $k_a$  (scale the axial active length) and  $N_t$  (scale the number of turns). The default active length of IMs in the database is 200mm, and the number of turns is 1. The optimizer will find the optimal machine length and number of turns, together with the designed inverter and transmission, to minimize the predefined cost function. The optimizer will assess each IM in the database, and any powertrain that cannot meet all the vehicle requirements will be discarded. Ultimately, the optimal solution for the vehicle with the lowest total cost will be selected.

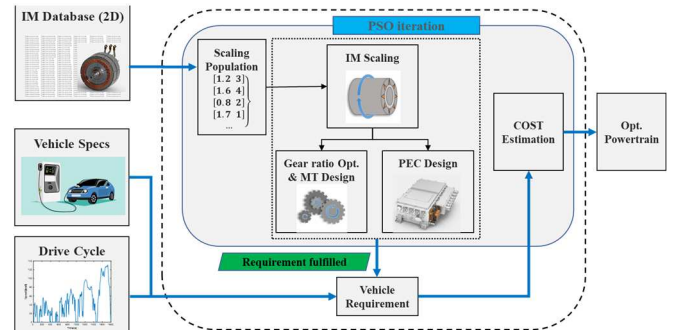


Fig. 11. Optimization methodology

### D. Optimization Results

The weighting factor ( $k_c$ ) of 0.5 has been established, indicating that the IM cost and vehicle operating cost are given equal importance. By optimizing 900 IMs, the powertrain



design solutions are presented in Fig. 12. Each circle in the figure represents the optimal powertrain configuration for a specific 2D IM geometry.

To ensure a fair sensitivity analysis, it is assumed beforehand that the current density and filling factor are consistent across all machines. Additionally, when creating the database, the total slot area is maintained at a constant value for IMs with varying  $q$  values. By keeping these variables constant, the sensitivity analysis can provide a more accurate and reliable assessment of the impact of changes in geometries on powertrain performance.

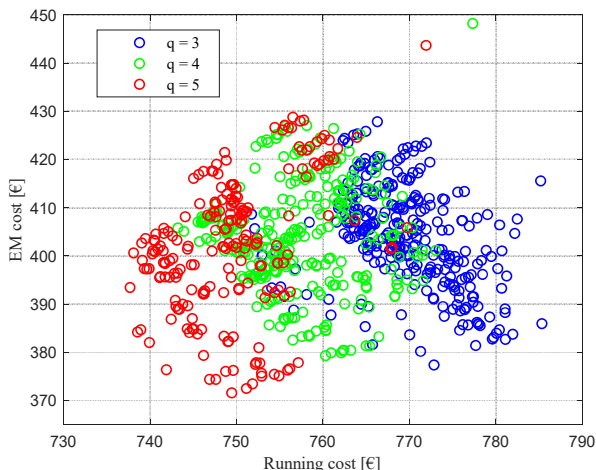


Fig. 12. Optimization results for all IMs

As depicted in Fig. 12, it is evident that the powertrains with a greater number of stator slots exhibit lower running cost, while the machine cost remains relatively constant. Based on the assumption that all machines can sustain the same current density, machines with 5 slots per pole per phase present feasible combinations of winding layers and parallel paths [15] that result into a phase current and therefore inverter sizing, closer to the actual requirements of the application. This translates into a lower running cost.

When designing the inverter, a higher input current results in increased losses, which can be seen in Fig. 13, therefore larger power modules are required.

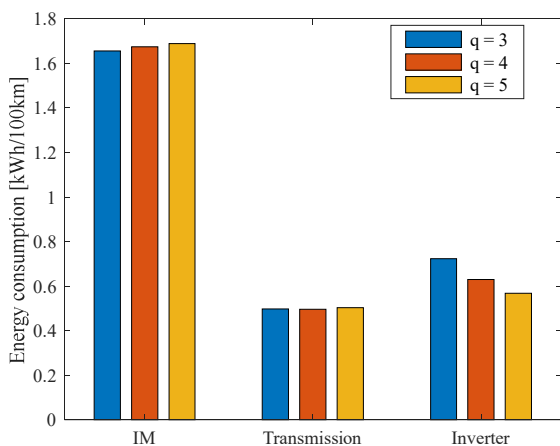


Fig. 13. Energy consumption of each component in three optimized powertrains with different number of stator slots

Variations between IMs with different slot sizes (relative slot size in Table I) can be seen in Fig. 14. By reducing the slot size while keeping the current density the same, the torque density of IMs is reduced, resulting in a larger machine to satisfy the vehicle requirements. Furthermore, the decrease in slot size results in an increase in winding resistance, leading to higher copper losses. Therefore, a higher running cost is expected.

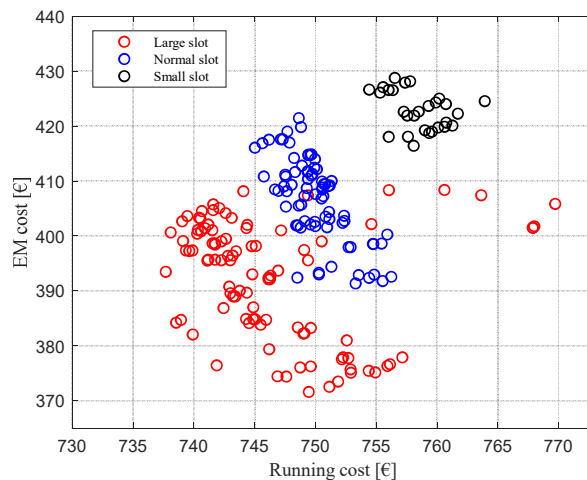


Fig. 14. Optimization results for IMs with five slots per pole per phase

However, a smaller slot can benefit from a better thermal performance, which is discussed in [16], thus a higher current density can be imposed to the stator winding. A deeper exploration with thermal analysis for the selection of an optimal slot should be considered in the future.

Finally, the optimal powertrain design is picked by the optimizer and the resulting efficiency map can be observed below in Fig. 14.

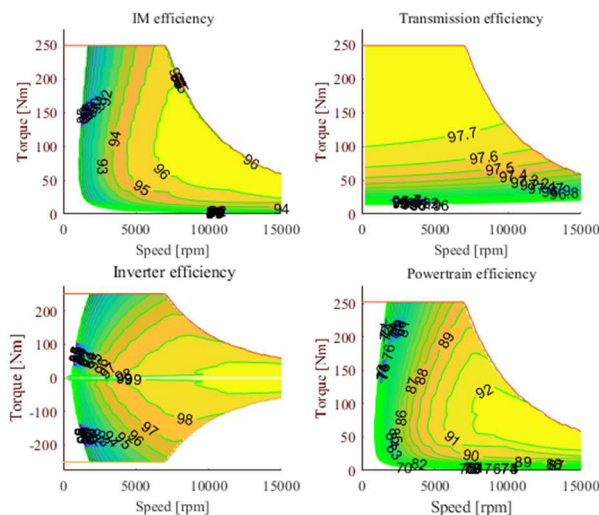


Fig. 15. Optimal powertrain performance

The powertrain design that provides the lowest total cost is presented in Table III.

TABLE III. OPTIMIZED POWERTRAIN DESIGN

Component	Parameters	Value
IM	Axial length	138 mm
	Num. of poles	4
	Num. of serial turns	10
	Num. of conductors per slot	8
	Num. of parallel paths	4
	Num. of slots per pole per phase	5
	Winding peak current density	16A/mm <sup>2</sup>
	Num. of rotor bars	74
	Ratio between total area of bars and rotor	0.12
	Peak power	181 kW
	Peak torque	251 Nm
Max speed	15000 rpm	
Transmission	Gear ratio	10.68
	Num. of teeth for gear stage 1	32/111
	Num. of teeth for gear stage 2	38/117
Inverter	Number of chips per bridge	3
	Single chip area	50 mm <sup>2</sup>

## V. CONCLUSION AND FUTURE WORK

This paper introduces an approach to optimizing an electric powertrain by incorporating induction machines. The proposed approach leverages computationally efficient methods to estimate and scale the electromagnetic performance of IMs, as explained in detail within the paper. While these methods have been previously discussed in literature, their integration into a complete powertrain optimization framework, including detailed transmission and inverter models, is unique and constitutes the primary contribution of this paper. A case study involving a database of 900 different 2D IM layouts has been presented, demonstrating the effectiveness of the proposed approach in optimizing electric powertrains using IMs. Future work will involve coupling the IM model with an existing PMSM model to optimize powertrains for dual-motor driven electric vehicles.

## ACKNOWLEDGMENT

The authors would like to express their gratitude to Swedish Energy Agency for supporting this research through grant number 50213-1.

## REFERENCES

- [1] Y. Tai, Z. Liu, H. Yu and J. Liu, "Efficiency optimization of induction motors using genetic algorithm and Hybrid Genetic Algorithm," 2011 International Conference on Electrical Machines and Systems, Beijing, China, 2011, pp. 1-4.
- [2] M. Tumbek, Y. Oner and S. Kesler, "Optimal design of induction motor with multi-parameter by FEM method," 9th International Conference on Electrical and Electronics Engineering (ELECO), Bursa, Turkey, 2015, pp. 1053-1056.
- [3] M. Lu, G. Domingues-Olavarria, F.J. Márquez-Fernández, P. Fyhr and M. Alaküla, "Electric Drivetrain Optimization for a Commercial Fleet with Different Degrees of Electrical Machine Commonality," *Energies* 2021, 14, 2989.
- [4] Spanoudakis, P, Moschopoulos, G, Stefanoulis, T, Sarantinoudis, N, Papadokokolakis, E, Ioannou, I, Piperidis, S, Doitsidis, L, Tsourveloudis, N.C. "Efficient Gear Ratio Selection of a Single-Speed Drivetrain for Improved Electric Vehicle Energy Consumption," *Sustainability* 2020, 12, 9254.
- [5] Koch, A, Nicoletti, L, Hermann, T and Lienkamp, M. "Implementation and Analyses of an Eco-Driving Algorithm for Different Battery Electric Powertrain Topologies Based on a Split Loss Integration Approach," *Energies* 2022, 15, 5396.
- [6] A. Merkert, T. Krone and A. Mertens, "Characterization and Scalable Modeling of Power Semiconductors for Optimized Design of Traction Inverters with Si- and SiC-Devices," in *IEEE Transactions on Power Electronics*, vol. 29, no. 5, pp. 2238-2245, May 2014.
- [7] G. Domingues-Olavarria, F. J. Márquez-Fernández, P. Fyhr, A. Reinap, M. Andersson and M. Alaküla, "Optimization of Electric Powertrains Based on Scalable Cost and Performance Models," in *IEEE Transactions on Industry Applications*, vol. 55, no. 1, pp. 751-764, Jan.-Feb. 2019.
- [8] H. Bydén, E. Boumiche, A. Leblay and M. Alakula, "Electro-thermal Models of Power Modules for Stochastic Optimization of Inverters," unpublished.
- [9] L. Jacob and H. O. Johanna, *Transmission Modeling for Optimization of Electric Powertrains*, Master thesis, Lund University, 2021.
- [10] J. Reinert, A. Brockmeyer and R. W. A. A. De Doncker, "Calculation of losses in ferro- and ferrimagnetic materials based on the modified Steinmetz equation," in *IEEE Transactions on Industry Applications*, vol. 37, no. 4, pp. 1055-1061, July-Aug. 2001.
- [11] Boldea, I, and Nasar. S.A. (2009). *The Induction Machines Design Handbook*. (2nd ed.), CRC Press.
- [12] M. Nell, J. Lenz and K. Hameyer, "Efficient Numerical Optimization of Induction Machines by Scaled FE Simulations," 2018 XIII International Conference on Electrical Machines (ICEM), 2018, pp. 198-204.
- [13] Nell, M., Lenz, J., & Hameyer, K. (2019). Scaling laws for the FE solutions of induction machines. *Archives of electrical engineering*, 68(3), 677-695.
- [14] Fyhr, P. *Electromobility: Materials and Manufacturing Economics*. Ph.D. Thesis, Lund University, Lund, Sweden, 2018.
- [15] S. Xue, M. Michon, M. Popescu and G. Volpe, "Optimisation of Hairpin Winding in Electric Traction Motor Applications," 2021 IEEE International Electric Machines & Drives Conference (IEMDC), Hartford, CT, USA, 2021, pp. 1-7.
- [16] Grunditz, Emma Arfa, et al. "Thermal capability of electric vehicle PMSM with different slot areas via thermal network analysis." *eTransportation* 8 (2021): 100107.